Sare Celik*, Aslan Deniz Karaoglan and Ismail Ersozlu

An Effective Approach Based on Response Surface Methodology for Predicting Friction Welding Parameters

Abstract: The joining of dissimilar metals is one of the most essential necessities of industries. Manufacturing by the joint of alloy steel and normal carbon steel is used in production, because it decreases raw material cost. The friction welding process parameters such as friction pressure, friction time, upset pressure, upset time and rotating speed play the major roles in determining the strength and microstructure of the joints. In this study, response surface methodology (RSM), which is a well-known design of experiments approach, is used for modeling the mathematical relation between the responses (tensile strength and maximum temperature), and the friction welding parameters with minimum number of experiments. The results show that RSM is an effective method for this type of problems for developing models and prediction.

Keywords: friction welding, AISI 316 stainless steel, Ck 45 unalloyed steel, response surface methodology

PACS. 81.Materials Science

DOI 10.1515/htmp-2014-0201
Received November 6, 2014; accepted February 6, 2015

Introduction

Friction welding is a solid-state welding process which is widely employed. Main advantages of friction welding are high material saving, low production time and the possibility of welding dissimilar materials. Economic and competitive production system has introduced the usage of different materials welded together in different phases of the production of the same part. Essential parameters of friction welding (FW) are friction pressure (*Pf*) and friction time (*tf*), upset pressure (*Pu*) and upset time (*tu*) and rotating speed (*n*) [1, 2]. The basic steps involved in FW are shown in Figure 1 [3]. Initially, one workpiece is rotated while the other is kept stationary as shown in Figure 1(a). When the appropriate rotational speed is reached, the two work pieces are brought together and axial force is applied as shown in Figure 1(b). Rubbing at the interface heats the workpiece locally which starts upsetting as shown in Figure 1(c). Finally, when rotation of one of the workpieces stops, this means upsetting is also completed (as in Figure 1(d)). The friction welding process is characterized by a narrow heat-affected zone (HAZ), the presence of plastically deformed material around the weld (flash) and the absence of a fusion zone. The relationship of parameters on continuous drive friction welding is shown in Figure 2 [1, 3].

Various researchers have investigated the relationship between mechanical work during FW and joint performance. When the literature is reviewed [4–6], it is understood that most of the published information on friction welding of dissimilar materials are focused on the microstructural characteristics, microhardness variations, phase formation and strength properties evaluation. There are also several studies that investigate the effect of welding parameters on mechanical properties of the material, welding zone, and the HAZ for AISI 304 stainless steel exist. The welding strengths and metallurgic properties of the joints were investigated using austenitic stainless steel (AISI 304) in [7–9]. Özdemir et al. [10] directed the effect of rotational speed on the interface properties of friction-welded AISI 304L to 4340 steel. Arivazhagan et al. [11] carried out to study the microstructure and mechanical properties of AISI 304 stainless steel and AISI 4140 low-alloy steel joints by different welding method.

AISI 316 is the second most popular steel of the stainless steel group. It has 20% consumption ratio in the whole stainless steel products. AISI 316 has good oxidation strength up to 870°C under the discrete service, and up to 925°C under the continuous service [12, 13]. Akbarimousavi et al. [14] carried out the study about friction welding of Cp-titanium and AISI 316L stainless

***Corresponding author: Sare Celik,** Department of Mechanical Engineering, Balikesir University, Balikesir, Turkey, E-mail: scelik@balikesir.edu.tr
Aslan Deniz Karaoglan, Department of Industrial Engineering, Balikesir University, Balikesir, Turkey, E-mail: deniz@balikesir.edu.tr
Ismail Ersozlu, Department of Mechanical Engineering, Army Academy, 06100 Ankara, Turkey, E-mail: iersozlu@gmail.com

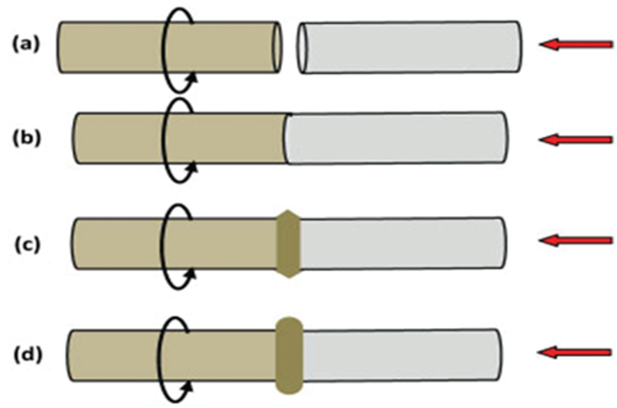

Figure 1: Basic steps in friction welding.

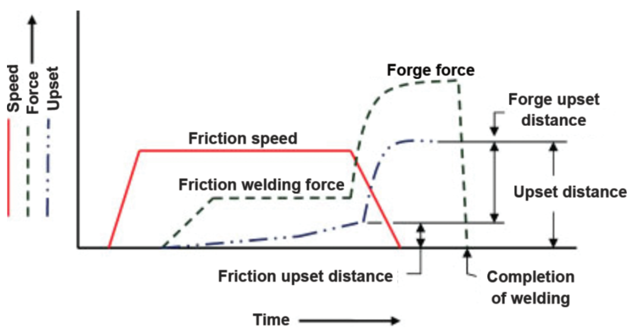

Figure 2: Parameters of continuous drive friction welding.

steel. The optimum operational parameters were obtained in order to achieve the weld tensile strength greater than the weak titanium material. Bhamji et al. [15] studied the linear friction welding of AISI 316L stainless steel. Analysis of the variation in delta ferrite, with different welding parameters, has produced some interesting insights into heat generation and dissipation during the process.

All the above-mentioned investigations were carried out on trial and other basis to attain optimum friction welding conditions. In spite of the fact that long tradition of industrial use of friction welding process, slight study has been reported so far to optimize the friction welding parameters to attain the maximum tensile strength. In the friction welding, the variation between theoretical and experimental values of flash features is analyzed by using ANN [16]. In the investigation of Paventhan et al. [17], an attempt was made to develop an empirical relationship to predict the tensile strength of friction-welded AA 6082 aluminum alloy and AISI 304 austenitic stainless steels joints, incorporating with the parameters that were mentioned above. Response surface methodology (RSM) was applied to optimize the friction welding process parameters to attain the maximum tensile strength of the joint. RSM of design of experiment (DOE) is used to analyze the results of rotary friction welding of steel with varying carbon [18].

Although a comprehensive review of the studies is presented for friction welding, there appears to be no study that presents the friction welding of the AISI 316 stainless steel and Ck 45 unalloyed steel which have a common usage area. This observation has been a motivation for the present work. Therefore, AISI 316 austenitic stainless steel and Ck 45 unalloyed steel are joined by friction welding in the present study and the mathematical relation is searched between the responses of friction welding process (tensile strength, max temperature) and the friction welding parameters (*tf*, *Pf*, *Pu*) by using RSM.

Rest of the paper is organized as follows: Materials and methods, Modeling of the system under study, Discussions and Conclusions.

Materials and methods

Friction welding experiments were carried out on a continuous drive friction welding machine controlled by the computer with a maximum load capacity of 101.736 kN and speed of rotation (3,000 rpm). The parent materials that were used in the present study are a commercial AISI 316 austenitic stainless steel and Ck 45 unalloyed steel for friction welding. The chemical compositions and measured tensile strengths of the parent materials are given in Table 1. Workpieces of both steels were machined in the form of bars with 10 mm diameter and 80 mm length. In this study, the parameters have been decided after some pre-experiments and by related literature search. Upset time (*tu*) and rotational speed were fixed at 20 s,

Table 1: The chemical composition of the materials used in the experiments (mass %).

Material	C (%)	P (%)	S (%)	Mn (%)	Si (%)	Mo (%)	Cr (%)	Ni (%)	Tensile strength (MPa)
AISI 316	0.032	–	0.018	1.464	0.378	2.098	17.06	10.63	663.55
Ck 45	0.39	0.026	0.009	0.646	0.212	0.033	0.213	0.113	715.2

and 3,000 rpm, respectively, while total friction times varied from 6 to 10; friction pressure were between 80 and 120 MPa, upset pressure range were from 120 to 200 MPa. Continuous drive friction welding machine was used to weld the joints (Figure 3). The macroscopic view of welded specimens is given in Figure 4. Tensile strength was measured to check the mechanical performance of the welding. The tensile tests have been prepared in accordance with the standards of EN 895, whereas the tests have been performed at the rate of 2 mm/min by Instron Corporation tension device. Tensile tests applied on welded specimens revealed that friction time, friction pressure and upset pressure, which are friction welding parameters, were effective on joint strength. Otherwise the temperature of the weld zone was measured using infrared temperature measurement device during welding process. Changes in the temperature of the welding parameters and their effects on the microstructure were observed.

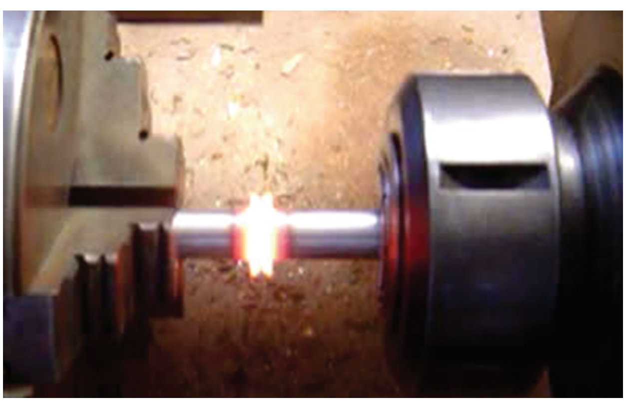

Figure 3: The specimens are joining by friction welding machine.

Figure 4: The macroscopic view of welded specimens.

Microstructures of the welded specimens were examined, by using optic and scanning electron microscope (SEM). In the welding area that was exposed to the friction welding, a materials transition region exists as well as the HAZ of the two main materials around this region. Figure 5 presents the main material of Ck 45 steel (Figure 5(a)) toward the HAZ of Ck 45 steel and the welding interface (Figure 5(b)) as well as the HAZ of AISI 316 steel (Figure 5(c)) and the main material of AISI 316 steel (Figure 5(d)) [19].

Different welding parameters have changed the width of welding zone and HAZ. The width of the welding zone expands with the increase of friction pressure and time. However, after a particular *tf* and *Pf* value the heated material at the welding zone carried out with a flash as can be seen in Figure 4 and both the temperature and the width of welding zone are decreased. The strength of the welded material is varied according to this situation.

Modeling of the system under study

This paper proposes an approach for predicting tensile strength from a second order polynomial equation obtained by modeling the relation between friction time (*tf*), friction pressure (*Pf*), and upset pressure (*Pu*) parameters by using RSM. RSM is a DOE technique which is used for prediction or optimization. In this study RSM is used for predicting the tensile strength (Rm) and maximum temperature of unexperienced factor combinations of *tf*, *Pf* and *Pu*. The advantage of using DOE techniques is modeling the relations between the factors (input variables) and the responses (output variables) with minimum number of experiments. When RSM is compared with other DOE techniques namely Taguchi method and factorial design, RSM has the advantage that it can give optimal solutions with decimals of factor levels while Taguchi gives the optimal combination of factors for the given factor levels and factorial design is appropriate for systems those can be modeled by first-order polynomials.

In this study, RSM was performed to establish the mathematical relationship between the responses (tensile strength and maximum temperature) and the input parameters (*tf*, *Pf* and *Pu*). For the modeling, 10 experiments are carried out by using actual values of *tf*, *Pf* and *Pu* which are given in Table 2. Because of the nonlinear relations between the mentioned factors, a full quadratic mathematical modeling that was based on RSM is carried out. Eq. (1) shows the general second-order polynomial response surface mathematical model (full quadratic model) for the experimental design:

$$Y = \beta_0 + \sum_{i=1}^{n} \beta_i X_i + \sum_{i=1}^{n} \beta_{ii} X_i^2 + \sum_{i<j}^{n} \beta_{ij} X_i X_j + e \qquad (1)$$

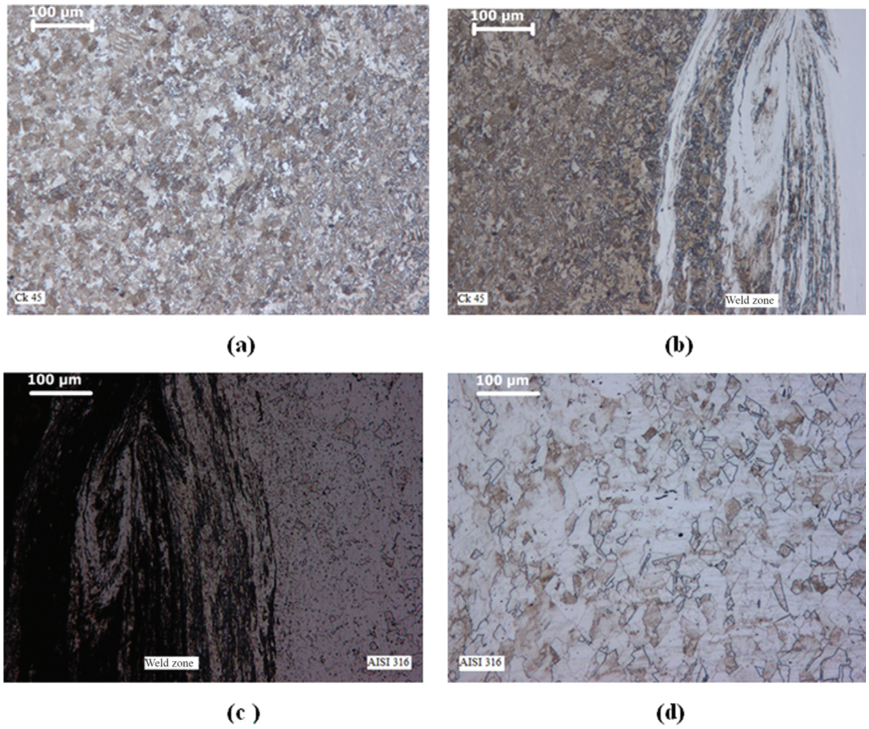

Figure 5: Optic microstructures of welded sample in the different zones.

Table 2: List of actual and corresponding values of *tf*, *Pf* and *Pu*.

Level	Low	Medium	High
tf	6	8	10
Pf	80	100	120
Pu	120	160	200

where Y is the corresponding response, X_i and X_j are values of the ith and jth input parameters; terms β_0, β_i, β_{ii} and β_{ij} are the regression coefficients; i and j are the linear and quadratic coefficients and e is the residual experimental error [20, 21]. Randomized experimental runs are carried out to minimize the error. MINITAB 16 statistical package is used to establish mathematical models for R_m and maximum temperature.

According to the experiments presented in Table 3, mathematical model that was based on RSM for predicting the response tensile strength has been established with 95% confidence and is represented in the following regression eq. (2) with R^2 value (coefficient of determination) of 99.999:

$$R_m = 5526.7 - 495.4tf - 82.71625Pf + 6.355Pu + 11.2tf^2 + 0.25506Pf^2 - 0.02544Pu^2 + 3.04125tf\,Pf + 0.2675tf\,Pu + 0.04563Pf\,Pu \quad (2)$$

Table 3: Design of experiments matrix with the observed responses.

tf (s)	*Pf* (MPa)	*Pu* (MPa)	R_m (MPa)
6	120	160	392.55
10	80	200	659.3
8	100	120	192.9
8	80	200	653.3
6	120	200	563.65
10	80	160	518.4
8	100	160	430.3
6	100	120	197.65
10	100	120	277.75
8	120	120	256.95

$$\text{Max temperature} = -3129 + 239tf + 49.55Pf + 7.875Pu - 4tf^2 - 0.135Pf^2 + 0.00438Pu^2 - 1.275tf\,Pf - 0.2625tf\,Pu - 0.06875Pf\,Pu \quad (3)$$

By using eq. (2), the surfaces and contours of response for tensile strength are plotted in Figures 6–8. It is clearly observed from Figures 6 to 8 that at the welding process of AISI 316 and Ck 45, tensile strength is highly affected from *Pu*. When the pairs of *Pu*-*tf* and *Pu*-*Pf* are considered together, it is observed that the effects of *tf* and *Pf* are quite low when they are compared to the effect of *Pu* on

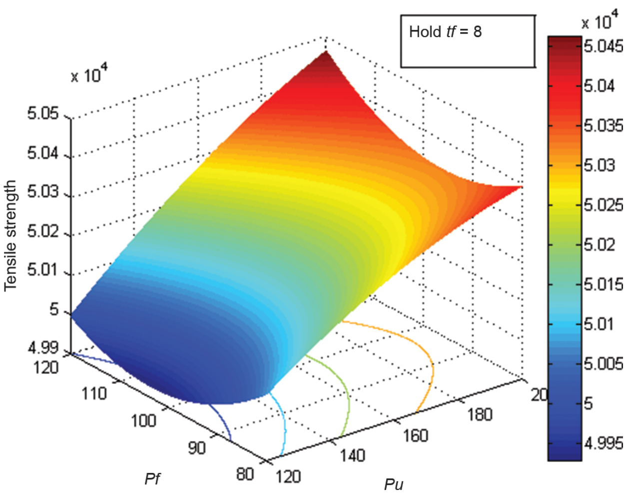

Figure 6: Surface plot of tensile strength versus *Pf* and *Pu*.

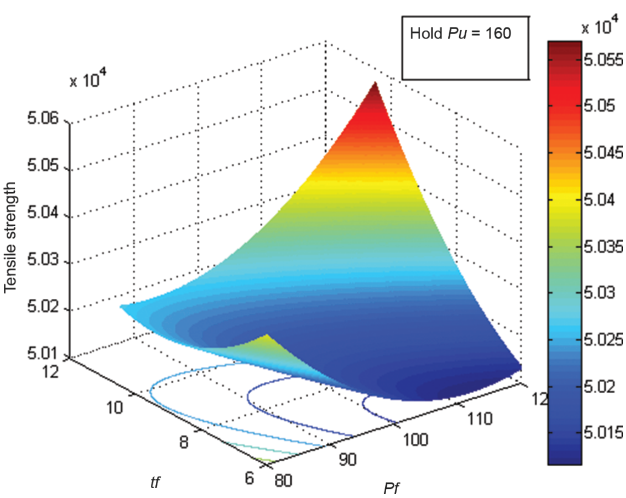

Figure 7: Surface plot of tensile strength versus *tf* and *Pf*.

tensile strength. *tf* and *Pf* together affect the tensile strength in various aspects. During the welding process, in the case of short friction times it has been observed that the tensile strengths were low, since the required temperature is not reached by the material for joining. Especially, when both the friction time and the friction pressure are low, a good welding strength was not achieved due to the lack of sufficient heat and material transition. However, after a critical level of parameters much deformation and length contraction are observed, and the welding strength is decreased. When *Pu* is holded at lower levels, forming fractures at the interfaces of welding is expected.

By using eq. (3), the surfaces and contours of response for maximum temperature are plotted in Figures 9–11. During the welding process, the maximum temperatures (995–1,072°C) was reached between 7 and 12 s. (The first 2 s have been accepted as a preparation time.) Heat increases rapidly. From that point forward, even though the rotation and *Pf* resume, the temperature rising speed slows down. The reason for this situation is the decrease of the friction coefficient caused by the warming up of the specimens [22] and the existence of the plastic deformation. Applying different friction pressures affected the reaching time of different welding temperature levels, which is proportional to the increase of pressure. It is observed that the maximum weld temperature did not exceed the hot deformation temperature. But after welded specimens, reaching the maximum weld temperature, continuous friction pressure and rotational process increase the deformation of the specimens, but were in no relation to *Pu* and temperature. It is clearly observed from Figures 9 to 11 that at the welding process of AISI 316 and Ck 45, two friction welding parameters,

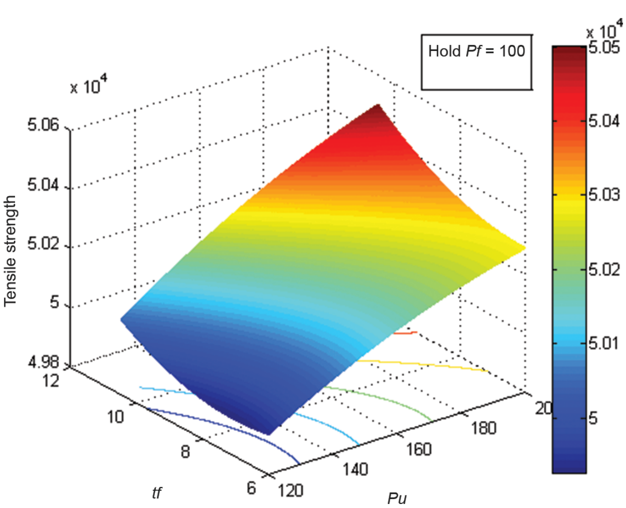

Figure 8: Surface plot of tensile strength versus *tf* and *Pu*.

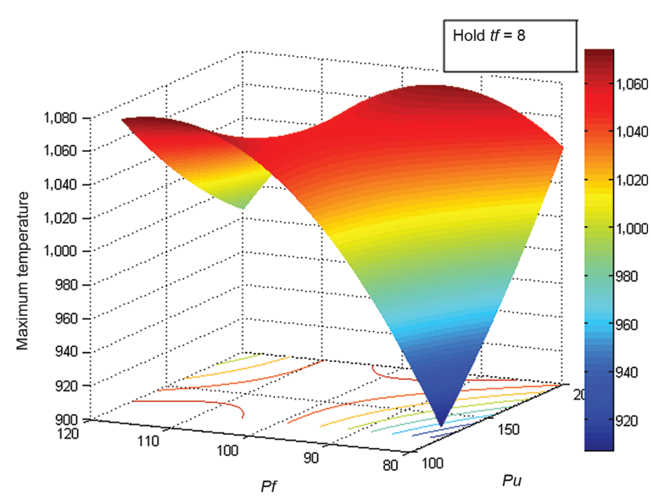

Figure 9: Surface plot of maximum temperature versus *Pf* and *Pu*.

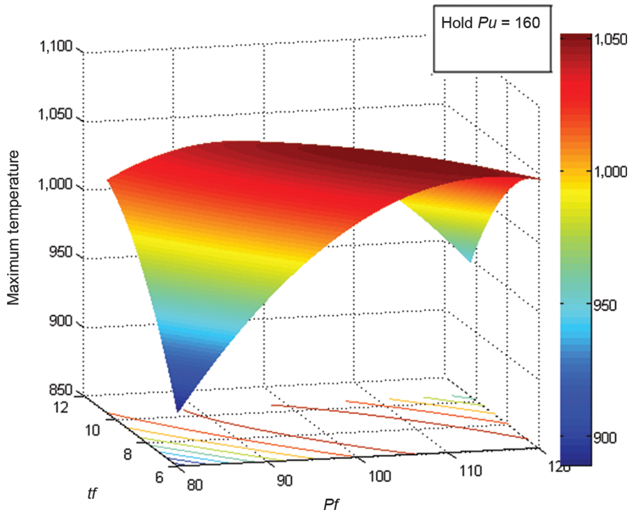

Figure 10: Surface plot of maximum temperature versus *tf* and *Pf*.

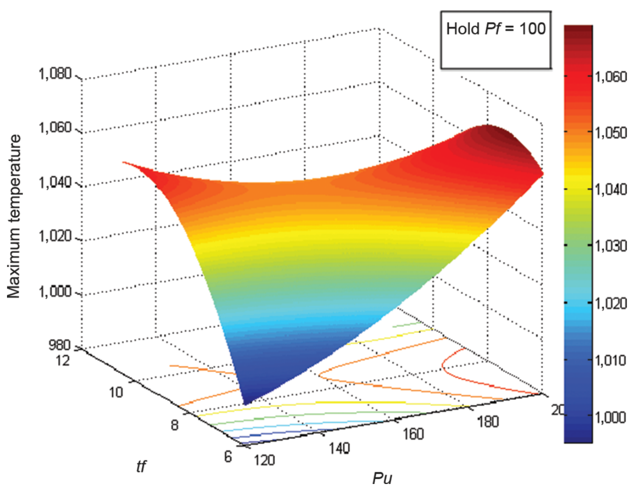

Figure 11: Surface plot of maximum temperature versus *tf* and *Pu*.

which are *Pf* and *tf*, affected the heat of the weld zone significantly. It is observed that the increase at temperature is less effected from the upset pressure when it is compared with the effects of *tf* and *Pf*.

The results predicted from the mathematical model that were given in eqs (2) and (3) are compared to those obtained by experiments in Table 4 for four sets of check data.

It can be concluded from the results that predictions can perform with an acceptable error ratio with less effort by using RSM.

Results and discussion

Austenitic stainless steels (such as AISI 316) are suitable for welding because of having high toughness besides having ductility and not exhibiting hardening at the HAZ. The carbide can only be decomposed at the welding seam that is heated up to the critical temperature and cooling down slowly. Having more than 450°C welding temperature causes comprising chrome carbide (Fe, $Cr_{23}C_6$). This chrome carbide is composed of 90% chrome, so a few carbons at the edge of grain boundaries decrease the chrome at the round of the austenite grains. As a result of this reaction, corrosion occurs at the grain boundaries which have insufficient chrome, when the material situated at a corrosive environment [23]. For this reason welding time and the maximum temperature have great importance at austenitic stainless steels. Friction welding disposes these negations under the pressure with low temperature when compared with the melting welding and short heating and cooling times.

By the determined friction welding parameters, the AISI 316 and Ck 45 steels have been welded successfully through applying the friction welding method. Optimum friction welding parameters were determined in the experimental studies in the joining process of AISI 316 austenitic stainless steel and Ck 45 steel. The highest tensile strength, which is 702.15 MPa, was 5.8% more than that of the parent material (AISI 316: 663.53 MPa). When the literature is reviewed, it is observed that the friction welding of the AISI 316 stainless steel and Ck 45 unalloyed steel has not been searched in welding parameters of friction time (*tf*), friction pressure (*Pf*) and upset pressure (*Pu*) together. The results demonstrated in the present study are new in the area.

The RSM model given in the previous section provides researchers to predict optimum combination of

Table 4: Confirmation tests.

tf	*Pf*	*Pu*	R_m (MPa)			Max. temperature (°C)		
			Exp.	Fitted	PE (%)	Exp.	Fitted	PE (%)
10	100	200	702.15	713.95	1.65	1,072	1,041	2.98
6	100	200	542.8	548.25	0.99	1,001	1,061	5.66
10	100	160	580.4	536.55	8.17	1,040	1,043	0.29
6	100	160	380.95	413.65	7.91	995	1,021	2.55

welding parameters for the presented tensile strength (R_m) values and maximum process temperature to the mathematical model that would be expected from the results of experiment, even for the numerous combinations of these experimental results.

In the present paper, it is observed that the given mathematical model produces acceptable results when compared to the experimental studies in this area. The average differences between the experimental and modeled results for each response ranged between 0.29% and 5.66% for confirmation tests. By using experimental design presented in the present study, with only 10 experiments an effective second-order full quadratic RSM model is obtained and by using this model the other combinations of experiments which were not performed can be predicted accurately with a confidence interval, which brings time and cost minimization.

Conclusion

The objective of this paper was to use the RSM – which is a collection of mathematical and statistical techniques used for designing the experiments – for predicting the tensile strength depending on various welding parameter combinations. By using RSM, an empirical relationship was developed to predict tensile strength and maximum temperature of friction welded AISI 316 stainless steel and Ck45 unalloyed steel. The developed mathematical models can be effectively used to predict the tensile strength of friction welded joints at a confidence level of 95%. The *Rm* and maximum temperature are predicted with maximum 8.17% and 5.66% error, respectively, at confirmation tests. The results demonstrated in the present study shows that RSM is an effective tool for this purpose.

Nomenclature

tf	Friction time (s)
Pf	Friction pressure (MPa)
tu	Upset time (s)
Pu	Upset pressure (MPa)
R_m	Tensile strength (MPa)
Y	The corresponding response
X_i, X_j	Values of the *i*th and *j*th input parameters
β_0	Constant of regression equation
β_i	Regression coefficients of linear terms
β_{ii}	Regression coefficients of square terms
β_{ij}	Regression coefficients of interactions
e	The residual experimental error of the *u*th observation

Acknowledgments: The authors would gratefully like to thank the editor and the anonymous referees whose valuable suggestions lead to improved organization of this paper.

References

[1] AWS, Welding Handbook, Welding Processes, 8th edn, American Welding Society Inc. (AWS), Miami (1997), pp. 739–761.
[2] S.D. Meshram, T. Mohandas and R.G. Madhusudhan, J. Mater. Process Technol., 184 (2008) 330–337.
[3] M.B. Uday, M.N. Ahmad Fauzi, H. Zuhailawati and A.B. Ismail, Sci. Technol. Weld. Joi., 15 (2010) 534–558.
[4] G.E. Linnert, Welding Metallurgy, Carbon and Alloy Steels, 4th edn, American Welding Society (AWS), Miami (2003), pp. 444, 593–607.
[5] S. Celik and I. Ersozlu, Mater. Des., 30 (2009) 970–976.
[6] AWS, Welding, Design, Procedures and Inspection, Department of the Army Technical Manual TM 5-805–7, Washington, DC (1985), pp. 4–1, 4–7.
[7] M. Sahin, Mater. Des., 28 (2007) 2244–2250.
[8] S. Celik, D. Dinc, R. Yaman and I. Ay, Prakt. Metallogr. Pr. M., 47 (2010) 188–205.
[9] P. Sathiya, S. Aravindan and A.N. Haq, Int. J. Adv. Manuf. Tech., 26 (2005) 505–511.
[10] N. Ozdemir, F. Sarsılmaz and A. Hascalık, Mater. Des., 28 (2007) 301–307.
[11] N. Arivazhagan, S. Singh, S. Prakash and G.M. Reddyb, Mater. Des., 32 (2011) 3036–3050.
[12] G. Krauss, Steels Processing, Structure and Performance, ASM International Materials Park, Ohio (2005), pp. 141–145, 495–531.
[13] B.L. Bramfitt and A.O. Benscoter, Metallographer's Guide Practices and Procedures for Irons and Steels, ASM International Materials Park, Ohio (2002).
[14] S.A.A. Akbarimousavi and M. GohariKia, Mater. Des., 32 (2011) 3066–3075.
[15] I. Bhamji, M. Preuss, P.L. Threadgill, R.J. Moat, A.C. Addison and M.J. Peel, Mat. Sci. Eng. A Struct., 528 (2010) 680–690.
[16] P. Sathiya, S. Aravindan, A.H. Noorul and K. Panneerselvam, Ind. J. Eng. Mater. S., 13 (2006) 37–44.
[17] R. Paventhan, P.R. Lakshminarayanan and V. Balasubramanian, Trans. Nonferrous Met. Soc., 21 (2011) 1480–1485.
[18] N.S. Kalsi and V.S. Sharma, Int. J. Adv. Manuf. Tech., 57 (2011) 957–967.
[19] S. Celik and I. Ersozlu, High Temp. Mater. Proc., 33–2 (2013) 161–170.
[20] D.C. Montgomery, Design and Analysis of Experiments, 5th edn, John Wiley &Sons, Inc., New York, NY, 2001.
[21] M. Demirtas and A.D. Karaoglan, Energ. Convers. Manage., 56 (2012) 104–111.
[22] Labthink Instruments Co. Material Friction Coefficient and Temperature, <http://www.labthink.cn/service/show558.html>, (2006).
[23] G. Krauss, Steels Processing, Structure and Performance, ASM International Materials Park, Ohio (2005).